ADVANCED MATERIALS
www.advmat.de

Designing Ultratough Single-Network Hydrogels with Centimeter-Scale Fractocohesive Lengths via Inelastic Crack Blunting

Jie Ma, Xizhe Zhang, Daochen Yin, Yijie Cai, Zihang Shen, Zhi Sheng, Jiabao Bai, Shaoxing Qu, Shuze Zhu, and Zheng Jia**

Fractocohesive length, defined as the ratio of fracture toughness to work of fracture, measures the sensitivity of materials to fracture in the presence of flaws. The larger the fractocohesive length, the more flaw-tolerant and crack-resistant the hydrogel. For synthetic soft materials, the fractocohesive length is short, often on the scale of 1 mm. Here, highly flaw-insensitive (HFI) single-network hydrogels containing an entangled inhomogeneous polymer network of widely distributed chain lengths are designed. The HFI hydrogels demonstrate a centimeter-scale fractocohesive length of 2.21 cm, which is the highest ever recorded for synthetic hydrogels, and an unprecedented fracture toughness of ≈13 300 J m^{-2}. The uncommon flaw insensitivity results from the inelastic crack blunting inherent to the highly inhomogeneous network. When the HFI hydrogel is stretched, a large number of short chains break while coiled long chains can disentangle, unwind, and straighten, producing large inelastic deformation that substantially blunts the crack tip in a plastic manner, thereby deconcentrating crack-tip stresses and blocking crack extension. The flaw-insensitive design strategy is applicable to various hydrogels such as polyacrylamide and poly(N,N-dimethylacrylamide) hydrogels and enables the development of HFI soft composites.

1. Introduction

Soft materials such as hydrogels and elastomers have been widely used as flexible wearable devices,[1] artificial organs for tissue engineering,[2] and soft robotics.[3] In these applications, soft materials are often subjected to large deformation and are thus susceptible to crack propagation. To enhance the crack resistance, toughening hydrogels has been a focal topic in the field of hydrogel development, with various hydrogels possessing enhanced fracture toughness over their conventional counterparts being developed in the past decade. Examples include double-network hydrogels,[4] highly entangled hydrogels,[5] hydrogels with force-reactive extensible chains,[6] and multi-length-scale hierarchical poly(vinyl alcohol) hydrogels.[7] Nevertheless, even for tough hydrogels, the introduction of flaws—which is often inevitable during the fabrication or sometimes required by specific applications [8]—can markedly reduce their stretchability and other ultimate properties.[9] Notably, the stretchability of elastomers and gels can be insensitive to flaws (i.e., the stretch at break does not reduce when a flaw is introduced) in the sample when the flaw length is relatively small compared to a material-specific length—the fractocohesive length,[10] which is defined as the ratio of the fracture toughness to the work of fracture. Obviously, the larger the fractocohesive length, the more flaw-tolerant and crack-resistant the hydrogel. Hence, it is of great significance to develop synthetic soft materials with large fractocohesive lengths, so that they can tolerate long flaws, resist crack propagation, and maintain their functionality in service.

The fractocohesive length of most synthetic soft materials to date is short—only around 1 mm (**Figure 1A**). Representative examples include state-of-the-art hydrogels such as hydrogels made of metal ion-clad picot fibers (p-Pep/Cu^{2+} hydrogels),[11] hierarchical poly(vinyl alcohol) (HA-PVA) hydrogel,[7] dry-annealed PVA hydrogel,[12] PAMPS-PAAm double-network hydrogel,[4b] regular polyacrylamide hydrogel,[13] and elastomers such as natural rubber,[10a] TPU,[9a] VHB,[10a] polyurethane,[10a] and ionic conductive elastomers.[14] Although various research works have focused on the design of tough soft materials,[5a,15] of which the fracture toughness has been greatly enhanced, these tough hydrogels barely possess large fractocohesive lengths since high fracture toughness does not necessarily lead to large fractocohesive length and high flaw insensitivity. For instance, the highly entangled hydrogels are tough and strong due to massive entanglements;[5a] however, the fractocohesive length is evaluated to be 2.39 mm based on their toughness and work of fracture reported. The classic PAMPS-PAAm double-network

J. Ma, X. Zhang, D. Yin, Y. Cai, Z. Shen, Z. Sheng, J. Bai, S. Qu, S. Zhu, Z. Jia
Key Laboratory of Soft Machines and Smart Devices of Zhejiang Province
Center for X-Mechanics
Department of Engineering Mechanics
Zhejiang University
Hangzhou 310027, China
E-mail: shuzezhu@zju.edu.cn; zheng.jia@zju.edu.cn

The ORCID identification number(s) for the author(s) of this article can be found under https://doi.org/10.1002/adma.202311795

DOI: 10.1002/adma.202311795

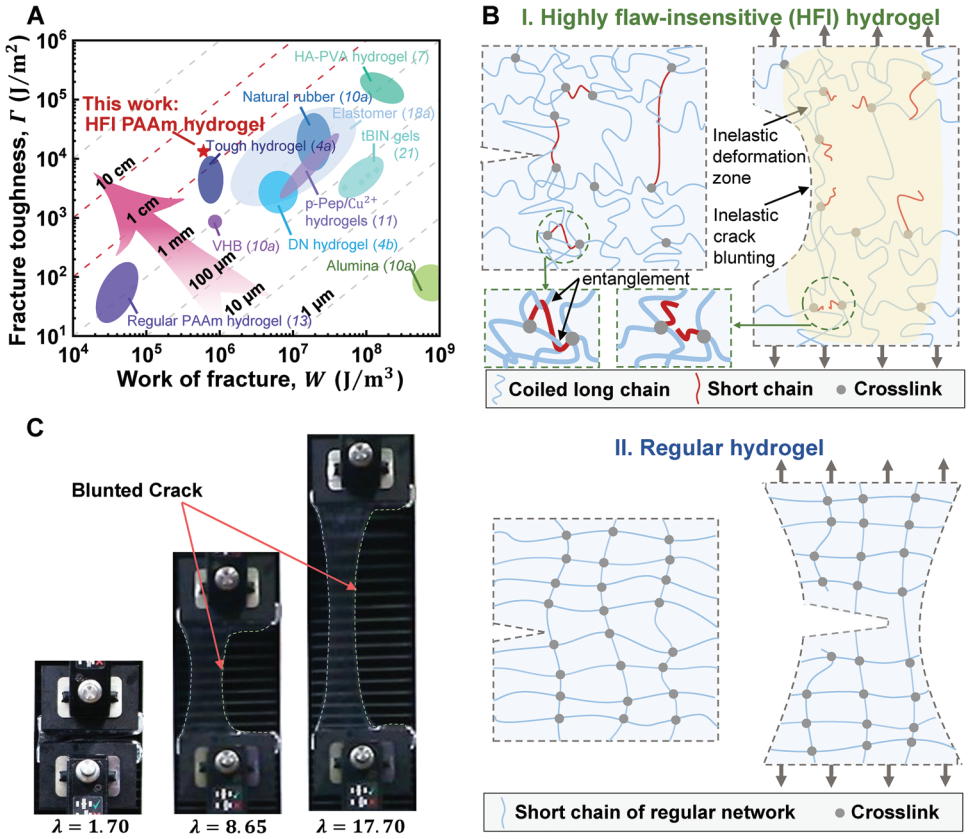

Figure 1. HFI PAAm hydrogels with a large fractocohesive length on the order of centimeters. A) The fractocohesive length of the HFI hydrogel and various materials. Existing synthetic soft materials exhibit fractocohesive lengths between 1 mm and 1 cm. The HFI hydrogel reported in this work has a fractocohesive length of 2.21 cm, outstripping nearly all existing synthetic soft materials. Notably, the fractocohesive length of the HFI PAAm hydrogel is enhanced by more than one order of magnitude compared to regular PAAm hydrogels. B) I. HFI hydrogel has an entangled inhomogeneous network containing polymer chains of widely distributed chain lengths—from long coiled chains to comparatively short ones. When the hydrogel is stretched, the breakage of short chains as well as the uncoiling of long chains collectively result in large inelastic deformation and pronounced inelastic crack blunting. A broken short chain also partly relaxes other chains entangled with it, contributing to the inelastic deformation that blunts the crack tip. II. Regular hydrogels are comprised of chains that are overall much shorter compared to those in HFI hydrogels due to dense crosslinks. In the deformed state, these short chains can be readily stretched taut simultaneously and build up high tension, causing chain breakage and the advancement of flaws, such that regular hydrogels are flaw-insensitive. C) Photographs demonstrating crack blunting of HFI hydrogels in the deformed configuration. The profile corresponding to the blunted crack surface becomes similar to the left free edge of the hydrogel, indicating the effect of the sharp crack has been largely attenuated.

hydrogel is considerably tough but only has a fractocohesive length of 0.432 mm.[16] Besides soft materials, the fractocohesive length of typical hard materials such as metals and ceramics is often below 100 μm.[10a,17] The usefulness of materials is determined by their ability to stretch without breaking. For the abovementioned synthetic soft materials whose fractocohesive length is about 1 mm, a flaw with the length of a few millimeters can markedly reduce the stretchability of the materials. The only hydrogel reported to date that exhibits a fractocohesive length reaching the level of 1 cm is PAAm-alginate double-network hydrogel.[9a] Synthetic hydrogels, especially single-network ones, with a fractocohesive length on the order of a few centimeters, however, are still lacking.

Here, using widely studied polyacrylamide (PAAm) hydrogel as a representative material system, we synthesize an ultratough highly flaw-insensitive (HFI) single-network hydrogel of a fractocohesive length of 2.21 cm via the inelastic crack blunting strategy, which sets the highest record for synthetic hydrogels to date (Figure 1A). The stretchability of the HFI hydrogel is insensitive to flaws of length of a few centimeters. In addition, the HFI hydrogels possess an unprecedented fracture toughness of ≈13 300 J m^{-2}. The HFI hydrogel is synthesized using unusually low amounts of crosslinkers with a high amount of water content. As we will show later with experimental measurements and molecular dynamics simulations, the synthesized hydrogel has an entangled inhomogeneous network that contains polymer chains with a broad range of chain lengths—from extremely long and highly coiled chains to comparatively short ones (Panel I of Figure 1B). It is such inhomogeneous networks consisting of both coiled long polymer chains and sacrificial short chains that render the hydrogel highly flaw-insensitive. When the HFI hydrogel is stretched, the polymer network transmits the high stress from the crack tip into the network, causing the breakage of a large number of short chains in a large area ahead of the crack, while the coiled long chains slide over each other—"lubricated" by the high content of water—to unwind and straighten, accommodating the large

applied elongation (Panel I of Figure 1B). The large inelastic deformation associated with this process gives rise to inelastic crack blunting, a phenomenon commonly observed in tough metals and alloys that is attributed to plastic deformation,[18] which can transit a sharp crack to a highly blunted notch (Figure 1C). The inelastic crack blunting can significantly attenuate the stress concentration at the crack tip and markedly reduce the sensitivity of hydrogels to the flaw. In addition, the usage of unusually low amounts of crosslinkers also leads to moderate amounts of entanglements [5a] (Panel I of Figure 1B). When short chains break, the deformation of long chains entangled with the short chains is relaxed, also contributing to the inelastic deformation that blunts the crack tip. In contrast, such mechanism is absent in regular hydrogels. Although regular hydrogels also possess an inhomogeneous network,[10b,c,19] chains in regular hydrogels have a narrower distribution of chain lengths and much shorter overall chain length due to dense crosslinks compared to HFI hydrogels (Panel II of Figure 1B), so the chains can hardly slide against each other due to the confinement of dense crosslinks and can readily be stretched taut. Therefore, these chains in front of the crack tip easily build up high tension and break almost simultaneously, causing the advancement of flaws, consequently rendering regular hydrogel flaw-sensitive.

2. Results and Discussion

To synthesize the HFI PAAm hydrogel, we use unusually low amounts of crosslinkers with normal amounts of water content and initiator. It is well known that synthesized hydrogels possess inhomogeneous networks of distributed chain lengths.[10b,c,19] The uncommonly sparse crosslinks result in inhomogeneous networks that contain very long and highly coiled polymer chains as well as relatively short chains (Figure 1B), as will be demonstrated later. For the precursor, we define M as the monomer-to-water molar ratio, C as the crosslinker-to-monomer molar ratio, and I as the initiator-to-monomer molar ratio. Unless otherwise noticed, we use $M = 0.0507$ and $I = 8.875 \times 10^{-4}$ throughout the experiment, which are normal amounts of water content and initiator used for synthesizing common PAAm hydrogels in the literature.[10b,c,20] We synthesize four PAAm hydrogels using precursors of different values of $C = 0.355 \times 10^{-4}$, 1.775×10^{-4}, 2.485×10^{-4}, and 3.195×10^{-4} in the ratio of 1: 5: 7: 9. For this reason, we name the four corresponding hydrogels 1C, 5C, 7C, and 9C hydrogels for simplicity. For example, the PAAm hydrogel of $C = 0.355 \times 10^{-4}$ is called 1C hydrogel and the hydrogel of $C = 2.485 \times 10^{-4}$ is 7C hydrogel. All the hydrogel samples with different crosslinker concentrations are well-cured. In particular, the unusually low crosslinker concentration of $C = 0.355 \times 10^{-4}$ (1C) can result in well-cured PAAm hydrogels that are chemically crosslinked and insoluble in deionized water (Figure S1, Supporting Information), while further decreasing C hardly leads to well-cured PAAm hydrogels. Dynamic mechanical analysis (DMA) test is conducted to characterize the gelation state of the 1C hydrogel, demonstrating that the 1C hydrogel is well-cured and behaves like an elastic solid rather than a viscous liquid (Figure S2, Supporting Information). Following the above recipe, all resultant as-synthesized hydrogels have a water content of ≈83.33 wt%, unless otherwise noticed.

We characterize the flaw-sensitivity of the as-synthesized PAAm hydrogels by uniaxially stretching precut samples along the height direction of the sample (Inset of **Figure 2A**). The hydrogel samples tested have overall dimensions of 1 cm in width (w), 5 cm in height (h), and 0.2 cm in thickness. Flaws of length a are made at the edge of the hydrogel perpendicular to the stretching direction (inset of Figure 2A). Stress–stretch curves of all samples under uniaxial tension are recorded. For each sample with given values of C and a/w, three samples are tested to ensure the replicability of the data (Figure S3, Supporting Information). We show that the 1C hydrogel samples are flaw-insensitive. The stretch at rupture λ_r of the 1C hydrogel without flaw (i.e., $a = 0$) is 18.14. As the normalized flaw length a/w increases to 0.6, 0.7, and 0.8, the stretch at rupture λ_r is 18.63, 18.74, and 19.05, respectively (Figure 2A). That is, the stretch at rupture λ_r of the 1C hydrogel does not reduce in the presence of flaws of various lengths, i.e., the hydrogel sample is flaw-insensitive. Figure 2B shows that the introduced flaw of $a/w = 0.8$ becomes highly blunted with a very large radius of curvature at the crack front under the subcritical stretch of $\lambda = 18.7$. In sharp contrast, 5C, 7C, and 9C hydrogel samples are apparently flaw-sensitive (Figure 2C–E). Take 7C hydrogels as an example. The stretch at rupture λ_r is 9.20 for $a/w = 0$ but reduces markedly to 2.16, 1.70, and 1.50 for $a/w = 0.3$, 0.5, and 0.8, respectively (Figure 2D). The sample demonstrates negligible crack blunting before the propagation of crack (Figure 2F). To this end, we call the 1C hydrogel highly flaw-insensitive hydrogel (i.e., the HFI hydrogel), and the other hydrogels, including 5C, 7C, and 9C, the regular hydrogels. We found the transition from HFI hydrogel to regular hydrogels happens around $C = 1.065 \times 10^{-4}$, which can be denoted as 3C (Figure S4, Supporting Information).

The flaw sensitivity of a material is closely related to the fractocohesive length, defined as the ratio of the fracture toughness Γ to the work of fracture W of the material.[10] In a sufficiently large hydrogel sample, a flaw shorter than the fractocohesive length has negligible effects on the ultimate stretchability of the hydrogel, as pointed out by Yang et al.[10b] To determine the fractocohesive length of the HFI hydrogel, we first measure the work of fracture W of the HFI hydrogel by rupturing dumbbell-shaped samples of no cuts in the uniaxial tension tests. Measurements using different sample dimensions yield a size-independent work of fracture W being ≈601.0 kJ m^{-3} (Figure S5, Supporting Information). Then, we measure the fracture toughness Γ by rupturing hydrogel samples of no cuts and long cuts (as long as 50% sample width), respectively, in the pure shear tests. The curves of precut samples with $a/w = 0.5$ and the corresponding curves of uncut samples (i.e., $a/w = 0$) are used to calculate the fracture toughness (Figure S6, Supporting Information). It is found that the measured fracture toughness rises with increasing dimensions of tested samples and saturates as the sample becomes sufficiently large (**Figure 3A**). Considering that the fracture toughness is also a material-specific quantity that should be independent of sample dimensions, the measured values in the saturated regime give the fracture toughness of the HFI hydrogel, about 13 300 J m^{-2} (Figure 3A and Table S1, Supporting Information), which is the highest fracture toughness reported for single-network hydrogels to date and is two orders of magnitude higher than that of regular PAAm hydrogels. The size-dependent fracture toughness indicates that the HFI hydrogel has a large

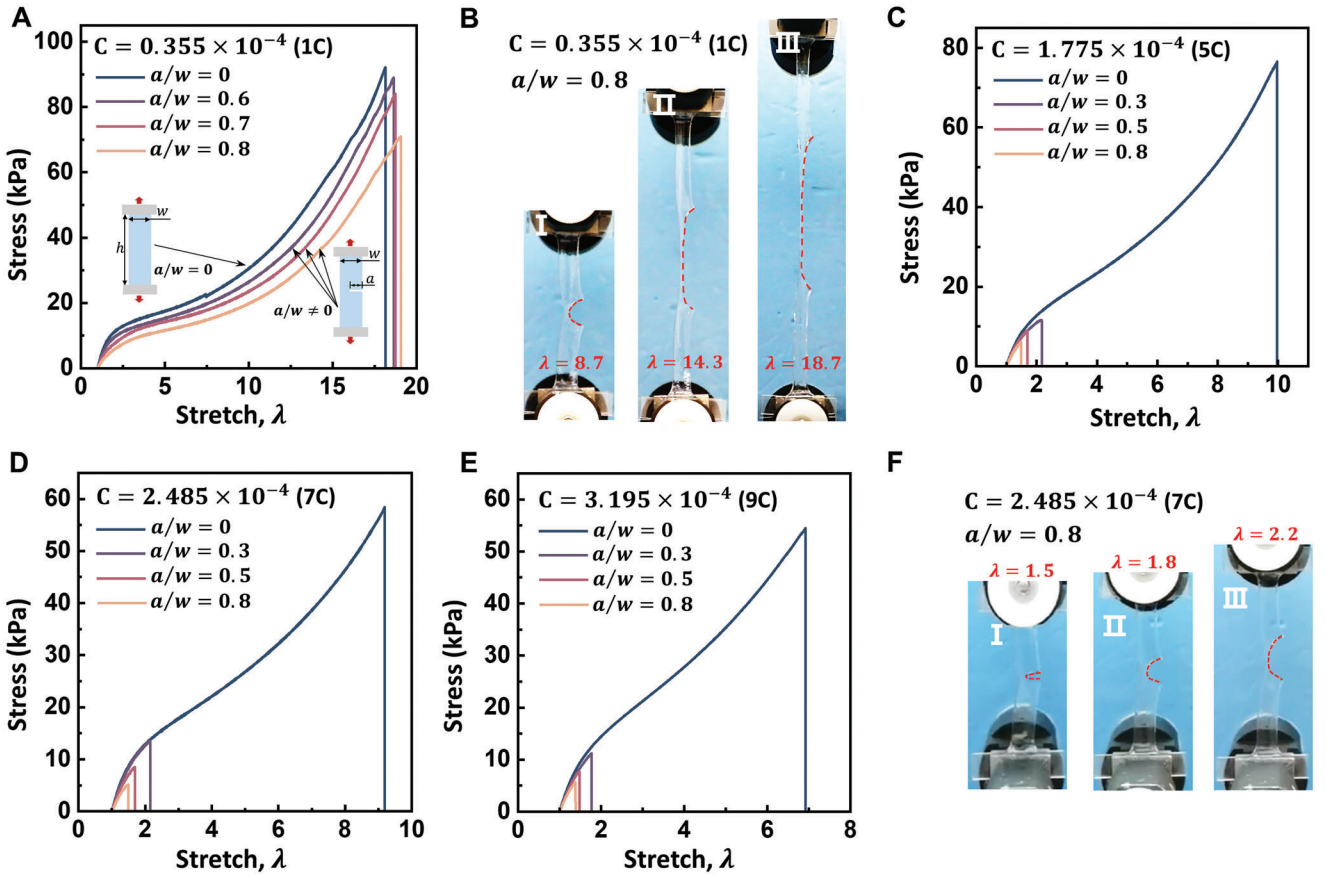

Figure 2. Flaw-sensitivity of highly HFI hydrogels and regular hydrogels. A) Stress–stretch curves of HFI hydrogels with $C = 0.355 \times 10^{-4}$ (1C). The 1C hydrogels are called HFI hydrogels since the stretchability is insensitive to flaws of any length in the sample. B) Photo images showing pronounced crack blunting in the 1C HFI hydrogel at large stretches. C–E) Stress–stretch curves of regular hydrogels with $C = 1.775 \times 10^{-4}$ (5C), 2.485×10^{-4} (7C), and 3.195×10^{-4} (9C), respectively. The stretchability of regular hydrogels is very sensitive to the introduction of flaws. F) The profile of crack front in 7C regular hydrogels before rupture.

inelastic fracture processing zone, the size of which scales with the fractocohesive length.[10b] When the characteristic length of the sample (i.e., the height of the sample in the pure shear tests) is small compared with the fracture processing zone, the fracture toughness increases with the dimension of the hydrogel. When the characteristic length of the sample is larger than the fracture processing zone, the fracture toughness becomes independent of the sample dimension. The transition from size-dependent to size-independent fracture toughness occurs at a characteristic length (i.e., the sample height) between 3 and 4 cm, which implies that the fractocohesive length of the HFI hydrogel is at this level since the size of the inelastic fracture processing zone scales with the fractocohesive length.

Based on the size-independent fracture toughness (Γ = 13 300 J m^{-2}) that is measured from sufficiently large samples and the work of fracture (W = 601 kJ m^{-3}) (Figure 3A; Table S1 and Figure S5, Supporting Information), the fractocohesive length is quantitatively calculated to be Γ/W = 2.21 cm (Figure 1A), setting the highest record for synthetic hydrogels so far—whose fractocohesive lengths are usually between 1 mm and 1 cm.[10a] We plot fractocohesive length data of various hydrogels and elastomers on the plane of fracture toughness Γ and work of fracture W (Figure 1A). The dashed slashes mark the constant values of the fractocohesive length Γ/W. The HFI PAAm hydrogel occupies the top left corner of the plane. The HFI hydrogel has a long fractocohesive length of 2.21 cm, which has not ever been realized before. This length is far higher than that of any state-of-the-art synthetic soft materials—from single-network to double-network—including p-Pep/Cu^{2+} hydrogels,[11] biomimetic interfacial-bonding nanocomposite (tBIN) hydrogels,[21] HA-PVA hydrogel,[7] dry-annealed PVA hydrogel,[12] PAAm-alginate tough hydrogel,[4a] PAMPS-PAAm double-network hydrogel,[4b] regular polyacrylamide hydrogel,[13] natural rubber,[10a] TPU,[9a] VHB,[10a] and polyurethane.[10a] The centimeter-scale fractocohesive length of the HFI hydrogels even reaches the level of natural soft tissues including bovine pericardium,[9a] rhinoceros dermal,[22] and liver capsule.[23] Notably, the HFI PAAm hydrogel is a single-network hydrogel, and its centimeter-scale fractocohesive length exceeds that of existing single-network hydrogels (including regular PAAm hydrogel) by more than one order of magnitude.

As discussed above, fractocohesive length—the ratio of the fracture toughness to the work of fracture—is one material constant that measures the flaw sensitivity of a material: a flaw

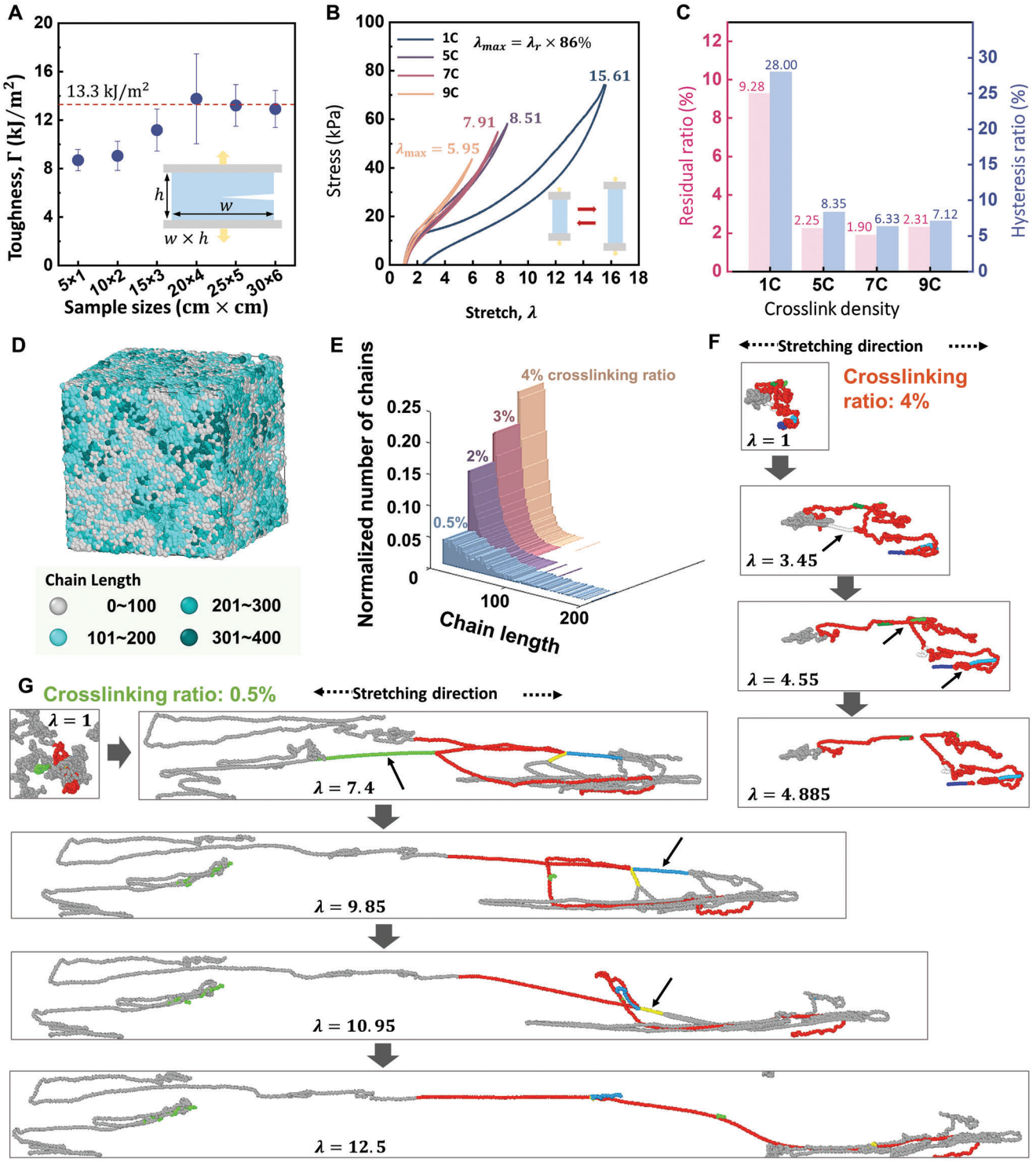

Figure 3. Fracture behavior and inelastic deformation of the HFI hydrogel. A) Fracture toughness of HFI hydrogels. By pure-shear tests, the fracture toughness of HFI hydrogels is measured by samples with sufficiently large dimensions, giving 13.3 kJ m^{-2}. B) Loading–unloading curves of HFI and regular hydrogels. Prior to unloading, all hydrogels are stretched to subcritical stretches, which are 86% of their stretches at rupture λ_r. C) Residual ratio and hysteresis ratio of HFI and regular hydrogels. The results indicate that the inelastic deformation of the HFI Hydrogel is much more pronounced than that of regular hydrogels. D) Coarse-grained molecular dynamics (CGMD) model of hydrogels with low crosslinking rate of 0.5%. E) CGMD-predicted chain length distribution of hydrogels with different crosslinking ratios, demonstrating a wide chain-length distribution in hydrogels with the crosslinking ratio of 0.5%. F,G) Examples of representative chain movements in hydrogels. The results illustrate short-chain breakage at similar stretches in hydrogels with a high crosslinking ratio of 4% prior to rupture (F), but sequential short-chain breakage as well as uncoiling/straightening of long chains in hydrogels with a low crosslinking ratio of 0.5% (G). The latter naturally leads to pronounced inelastic deformation. The colors are used to highlight different chains.

shorter than the fractocohesive length has negligible effects on the ultimate stretchability of the material.[10b] It is worth noting that there is another material constant that quantitatively characterizes the flaw sensitivity of a material, the flaw-insensitive length,[16,24] which scales with the fractocohesive length but is measured in a different way from the fractocohesive length. The method for determining the flaw-insensitive length is as follows: the stretchability of sufficiently large samples with different cut lengths is measured and recorded. The stretches at rupture of precut samples are almost the same as the values of uncut samples when the flaw is short, but become smaller than the values of uncut samples when the cut is long.[16] The transition takes place at a critical cut length, which is the flaw-insensitive length. To measure the flaw-insensitive length of the HFI hydrogel, we use the samples with dimensions of 20 cm in width and 8 cm in height (Figure S7, Supporting Information). Various flaw lengths are introduced to the samples. The stretches at rupture of the HFI hydrogel samples do not decline as the length increases up to 5 cm, indicating that the flaw-insensitive length of the HFI hydrogel is no less than 5 cm (Figure S7, Supporting Information). To date, flaw-insensitive length has been tested for only a few soft materials, including VHB,[25] Ecoflex,[25] regular PAAm hydrogels,[10b] and the PAMPS-PAAm double-network hydrogel,[16] with flaw-insensitive length ranging from microns to millimeters (Table S2, Supporting Information). As above noted, the flaw-insensitive length of the HFI hydrogel is on the order of centimeter scale, well exceeding reported values of typical soft materials, including that of the classic tough PAMPS-PAAm double-network hydrogel.

The flaw-insensitive behavior of the HFI hydrogels can be attributed to inelastic crack blunting and corresponding crack-tip stress deconcentration. To demonstrate the remarkable inelastic deformation behavior of HFI hydrogel, we load the HFI hydrogels and regular hydrogels to subcritical stretches—86% of their stretches at rupture shown in Figure 2—and unload (Figure 3B). For all hydrogels tested, we note that after unloading, the stretch at zero nominal stress is larger than 1, which is indicative of residual inelastic deformation. We regard the residual ratio, which is defined by the ratio of the residual strain to the maximum applied strain, as one measure of the inelastic deformation. For the HFI 1C hydrogel, the residual ratio due to inelastic deformation is 9.28% (Figure 3C), much larger than that of regular PAAm hydrogels—2.25% for the 5C hydrogel, 1.90% for the 7C hydrogel, and 2.31% for the 9C hydrogel. Moreover, the unloading curves of all PAAm hydrogels are below the loading curves (Figure 3B). The area under a loading curve is the work done by the load, and the area between the loading and unloading curve is the energy dissipated during loading and unloading. Hysteresis can be defined as the ratio of the energy dissipated to the work done, serving as another measure of the inelastic deformation of hydrogels. For the HFI hydrogel and other regular hydrogels of 5C, 7C, and 9C, the hysteresis is 28.00%, 8.35%, 6.33%, and 7.12% (Figure 3C), respectively. Under cyclic stretches, the 1C HFI PAAm hydrogels also exhibit significantly higher residual ratio and hysteresis ratio than those of regular PAAm hydrogels (Figures S8–S10, Supporting Information). The larger residual ratio and hysteresis of HFI hydrogels in comparison to regular hydrogels indicate more pronounced inelastic deformation in HFI hydrogels under deformation. In addition, under cyclic loads, stress–stretch curves of HFI hydrogels exhibit considerable hysteresis in the first cycle but remain almost unchanged in the subsequent cycles, indicating that the viscoelasticity of the HFI hydrogels is negligible (Figure S11, Supporting Information).

The significant inelastic deformation of HFI hydrogels results from a microscopic fact of polymer networks: real polymer networks are inhomogeneous, consisting of chains of unequal lengths, as revealed by series of experimental,[10b] theoretical,[26] and simulation studies;[26e,f] and sparser crosslinks may lead to wider chain length distribution.[27] To verify this molecular picture, coarse-grained molecular dynamics (CGMD) simulations are conducted on four representative hydrogel models with different crosslinking ratios of 0.5%, 2%, 3%, and 4%, which are defined as the number of crosslinks divided by the number of grains in the network model. Note that the HFI hydrogels are made with the unusually low amount of crosslinkers, such that the CGMD model with low crosslinking ratios of 0.5% corresponds to the HFI hydrogels, while models with crosslinking ratios of 2%, 3%, and 4% correspond to regular hydrogels. It can be found from CGMD simulations that hydrogels of 0.5% crosslinking ratios contain both highly-coiled long polymer chains and comparatively much shorter chains (Figure 3D and Figure S12, Supporting Information). Figure 3E shows the simulated chain length distribution of hydrogel models with different crosslinking ratios: The hydrogel of the low crosslinking ratio of 0.5% exhibits widely distributed chain lengths, containing not only many extremely long chains—a natural consequence of using small amounts of crosslinkers—but also, counterintuitively, a large number of very short chains, with the chain length distribution spanning more than an order of magnitude (Figure 3E). In stark contrast, hydrogels of high crosslinking ratios (i.e., 2%, 3%, and 4%) have much narrower distributions of chain lengths, with mostly very short chains as expected (Figure 3E and Figure S12, Supporting Information). Nuclear magnetic resonance (NMR) tests performed on crosslinked hydrogel systems also reveal that a lower concentration of crosslinker results in higher network inhomogeneity, which is in line with the findings from our CGMD simulations.[27] Figures 3F,G show the deformation of a small group of representative chains, revealed by CGMD simulations of stretching hydrogel of different crosslinking ratios. It is shown that as the hydrogel with the low crosslinking ratio of 0.5% is stretched, short chains (e.g., chains highlighted by green, blue, and yellow in Figure 3G) distributed throughout the network sequentially break, leading to the rearrangement of the intact long chains into longer chains (e.g., the red chain illustrated in Figure 3G). Figure S13A (Supporting Information) records the number of broken chains in the hydrogel model with the low crosslinking ratio of 0.5% as the function of applied stretch, further corroborating the sequential and continuing short chain breakage during stretching. The short-chain breakage and the uncoiling/straightening of extremely long chains at the microscopic scale collectively give rise to the large inelastic deformation of hydrogels with the low crosslinking ratio at the macroscopic scale. In sharp contrast, the short chains that constitute the hydrogel with a high crosslinking ratio of 4% break easily at similar stretches right before the rupture of the hydrogel (Figure 3F; Figures S13B,D, and S14, Supporting Information), resulting in minimal inelastic deformation prior to rupture of the hydrogel.

The entanglements formed due to the usage of unusually low amounts of crosslinkers in synthesizing the HFI hydrogel (1C) are also believed to contribute to the inelastic deformation that substantially blunts the crack. It is widely recognized that lower crosslinker concentration leads to smaller modulus and softer hydrogels.[5a] Here, we found that the modulus of the HFI PAAm hydrogel synthesized with the unusually low crosslinker concentration $C = 0.355 \times 10^{-4}$ (1C) is about 21.6 kPa (Figure S15, Supporting Information), very close to that of regular PAAm hydrogels with $C = 1.775 \times 10^{-4}$ (5C), 2.485×10^{-4} (7C), and 3.195×10^{-4} (9C), which are five, seven, and nine times that of the crosslinker concentration used for the 1C HFI PAAm hydrogel. Moreover, the modulus of the HFI PAAm hydrogel is also comparable to that of most regular PAAm hydrogels reported in the literature,[10b,c,13a,20,28] which is on the order of 10 kPa (Table S3, Supporting Information). The results indicate that the modulus of HFI hydrogels is not compromised by the uncommonly low crosslinker concentration, which signifies the existence of entanglements formed due to low crosslink density.[5a] Following Kim et al.,[5a] we assume that all crosslinkers in a precursor are incorporated into the polymer. Each crosslinker connects four chains and each chain has two ends. Hence, the average number of monomers per chain is $1/2C$, where C is the crosslinker-to-monomer molar ratio. For the HFI hydrogel, the average number of monomers per chain is $1/(2 \times 0.355 \times 10^{-4}) = 1.41 \times 10^4$—each chain has, on average, 1.41×10^4 monomers. Note that the modulus of the HFI hydrogel, of which $C = 0.355 \times 10^{-4}$, is similar to that of the 9C hydrogel, of which $C = 3.195 \times 10^{-4}$, indicating that the entanglements in the HFI hydrogel effectively shorten the polymer chains to $1/(2 \times 3.195 \times 10^{-4}) = 0.156 \times 10^4$ monomers. That is, each chain has entanglements equivalent to ≈10 cross-links. When the HFI hydrogels are stretched, before the short chains break, tension transmits along the chain and to many other long chains through entanglements. When the short chains break, the network relaxes the tension and deformation in many long chains that were entangled with the short chains, contributing to the inelastic deformation of HFI hydrogels.

The above physical picture can be applied to understand the unprecedented fractocohesive length of the HFI hydrogel. The inelastic deformation due to long-chain disentangling and unwinding induced by short-chain scission is more pronounced near the tip of existing flaws. From the macroscopic perspective, it is well known that inelastic deformation causes inelastic crack-tip blunting,[18b] i.e., the irreversible transition from a sharp crack to a highly blunted notch. Figure S16 (Supporting Information) demonstrates significant inelastic deformation around the crack tip in HFI hydrogels. After being stretched to a subcritical stretch of 18.63 and released, an initial round black mark ahead of the sharp crack tip in the HFI hydrogels becomes a narrow stripe along a widely open V-shaped notch (Figure S16A, Supporting Information), which suggests that significant inelastic deformation occurs around the crack tip in the HFI PAAm hydrogel. The inelastic deformation around the crack tip leads to inelastic crack blunting, where the initial sharp crack irreversibly turns into a highly blunted crack (Figure S16A, Supporting Information). The blunting of crack can significantly deconcentrate stresses at the tip of flaws. By contrast, the inelastic deformation around the crack tip in the regular 7C hydrogel is negligible, with the initial crack remaining sharp after being released from the subcritical stretch (Figure S16B, Supporting Information), suggesting a lack of stress attenuation mechanisms. From the microscopic perspective, chains in regular hydrogels have narrower chain length distributions and are much shorter than those in HFI hydrogels; they can hardly slide against each other due to the confinement of dense crosslinks. When the regular hydrogel is stretched, these chains on the crack plane easily build up high stresses and break (Figure S17A, Supporting Information), causing the advancement of flaws. In sharp contrast, coiled long polymer chains in HFI hydrogels can accommodate the large deformation near the tip of flaws by disentangling, decoiling, and sliding against each other, significantly deconcentrating high tension of chains and stresses at the flaw tips (Figure S17B, Supporting Information), thereby giving remarkable flaw insensitivity of the HFI hydrogels.

Fracture is a size-dependent phenomenon. Larger samples are more prone to crack advancement than smaller ones. Thanks to the unprecedented fractocohesive length, large-sized HFI hydrogels with characteristic lengths on the scale of centimeters can be insensitive to flaws contained in the sample. The fracture of materials is a result of the interplay between the characteristic length of the sample (i.e., the smallest relevant sample dimension and the flaw length) and the size of the fracture processing zone, which scales as the fractocohesive length. Therefore, the stretch at rupture of hydrogels is not only dependent on the flaw length, but also on the sample sizes. When the sample dimension is relatively small compared to the size of the fracture processing zone, a hydrogel is insensitive to flaws contained in the sample. Otherwise, the hydrogel becomes susceptible to the propagation of existing flaws and is sensitive to flaws contained in the sample. For this reason, it is widely recognized that large hydrogel samples tend to be sensitive to flaws. The stretchability of common hydrogel samples with characteristic length reaching ≈1 cm is sensitive to flaws introduced to the samples.[4a,10b,29] Here, we show that large HFI hydrogel samples with characteristic length up to ≈8 cm are flaw-insensitive, we test a series of HFI hydrogel samples, with the same sample width of $w = 20$ cm and thickness of 0.2 cm but varying heights of 6 and 8 cm, respectively (inset of **Figure 4C**). The samples with heights of 6 and 8 cm are flaw-insensitive with different flaw lengths (Figure 4A,B). In sharp contrast, 7C regular hydrogels with dimensions of 20 cm × 6 cm × 0.2 cm and precuts (length of cut is 5, 10, and 15 cm, respectively) all rupture at a very low stretch around 2, significantly lower than that of uncut samples, which is 8.68 (Figure 4C). In fact, regular PAAm hydrogel samples with even smaller dimensions are still sensitive to flaws (Figure 2C–E). Moreover, it is worth noting that double-network PAAm-alginate hydrogel—a well-known representative tough hydrogel with a fractocohesive length around ≈1 cm—with dimensions of 7.5 cm × 0.5 cm, which is much smaller than dimensions of HFI hydrogels in Figure 4A,B, is sensitive to flaws in it: Introducing a flaw reduces the stretchability of the PAAm-alginate hydrogel from 21 to 17, with an ≈19% reduction.[4a]

It is widely recognized that high water content often compromises the mechanical properties of hydrogels, since water negligibly transfers forces. Here, we find that high water content, counter-intuitively, is key to maintaining the flaw-insensitivity of HFI PAAm hydrogel. To demonstrate this, we synthesize hydrogels of various water content—from 75 to 84.62 wt%—by

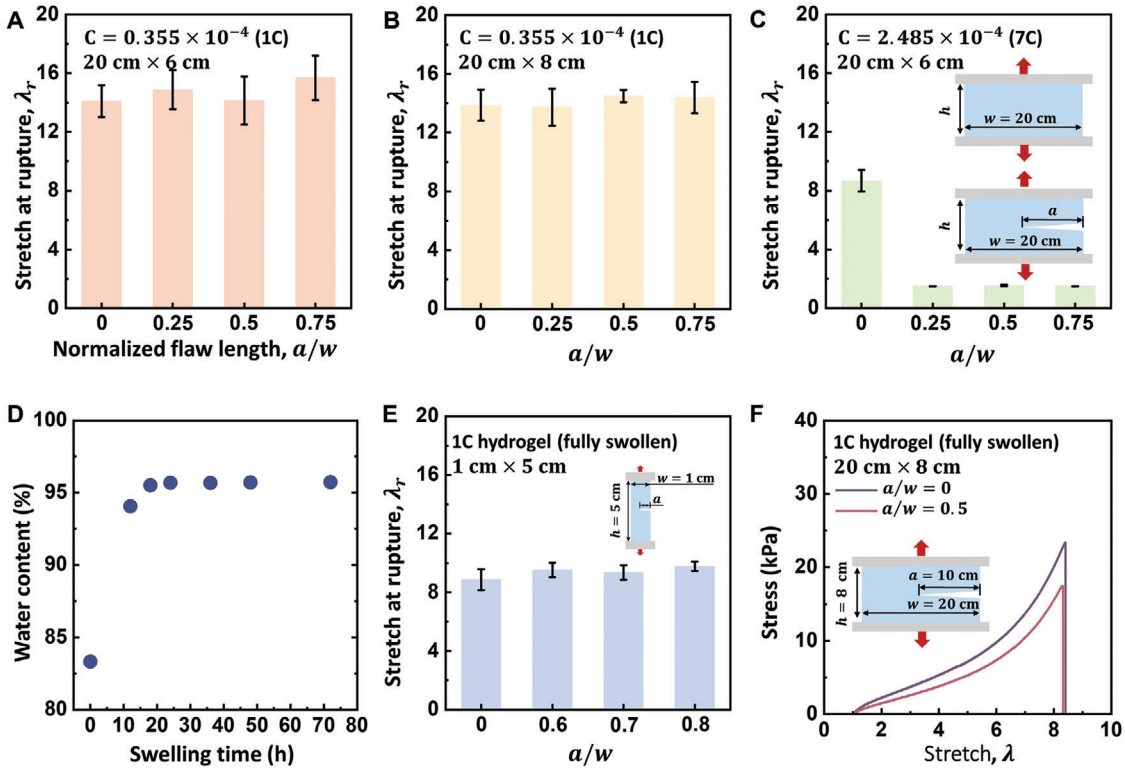

Figure 4. Flaw sensitivity of HFI PAAm hydrogel samples of large dimensions and in the fully swollen state. A,B) Stretch at rupture of HFI PAAm hydrogel samples with large dimensions of 20 cm × 6 cm and 20 cm × 8 cm, which are insensitive to flaws of different lengths. C) Flaw-sensitive stretch at rupture of regular PAAm hydrogel sample in the dimensions of 20 cm × 6 cm. D) Water content of HFI hydrogels immersed in water as a function of time. The water content gradually increases from 83.33 to 95.68 wt% in 24 h. E) Stretch at rupture of fully swollen HFI hydrogels with dimensions of 1 cm (width) × 5 cm (height) as a function of normalized cut length. F) Stress–stretch curves of fully swollen HFI hydrogel samples with dimensions of 20 cm (width) × 8 cm (height). The hydrogel sample is flaw-insensitive since the introduction of flaws does not lead to a decline in the ultimate stretchability.

changing the water content of the precursor solution. The hydrogel dimensions are fixed to 1 cm (width) × 5 cm (height) × 0.2 cm (thickness). It is found that hydrogel samples with high water content—no less than 76.47 wt%—are flaw-insensitive (Figure S18A–C), while samples with relatively low water content—less than 75 wt%—become flaw-sensitive (Figure S18D, Supporting Information). That is, the reduction in water content leads to a transition from flaw-insensitive to flaw-sensitive behavior. It is speculated that high water content can reduce the molecular interaction (i.e., friction) between polymer chains and facilitate the sliding and uncoiling of long chains, thus enabling large inelastic deformation and imparting high flaw-insensitivity to the hydrogel. Moreover, to test the flaw-sensitivity of fully swollen hydrogels (often with water content beyond 90 wt%) immersed in water environment, a working condition required by many applications, we put as-synthesized HFI hydrogel samples with initial water content of 83.33 wt% in deionized water. The hydrogel swells to equilibrium after the submersion in water, with the water content increasing gradually and eventually reaching a plateau level of 95.73 wt% at the fully swollen state (Figure 4D and Figure S19, Supporting Information). It is demonstrated that the fully swollen HFI PAAm hydrogel samples with in-plane dimensions of 1 cm (width) × 5 cm (height) and 20 cm (height) × 8 cm (width) are both insensitive to large flaws (Figure 4E,F), demonstrating that HFI hydrogel samples in its fully swollen state with an equilibrium water content of 95.73 wt% are still highly flaw-insensitive. It is speculated that the high water content facilitates the coiled long polymer chains to slide over each other, unwinding and straightening them, resulting in large inelastic deformation and large flaw insensitivity. Notably, despite the unusually low amount of cross-linker used in the synthesis of the HFI PAAm hydrogels, the measured water content of fully swollen HFI PAAm hydrogels (95.73 wt%) is comparable to that of fully swollen regular PAAm hydrogels using a normal amount of crosslinkers (Table S4, Supporting Information), which indicates the formation of entanglements in the HFI PAAm hydrogel, as speculated above. The entanglement compensates for the influence of low crosslinking density, resulting in a swelling ratio that is comparable to, rather than much higher than, those reported in the literature for regular PAAm hydrogels. As expected, uniaxial tension tests reveal that the fully swollen HFI hydrogel possesses a lower modulus of 4.57 kPa, which is lower than that (≈21.6 kPa) of the as-synthesized HFI hydrogel (Figure S20, Supporting Information).

In terms of application, the HFI PAAm hydrogel can be applied to enhance the flaw-resistance of regular hydrogels via fabricating hydrogel composites, which consist of alternating strips of HFI hydrogel and regular hydrogel. We demonstrate the strategy by fabricating a model composite, with the 7C regular hydrogel—which is flaw-sensitive—and 1C HFI hydrogel arranged in an

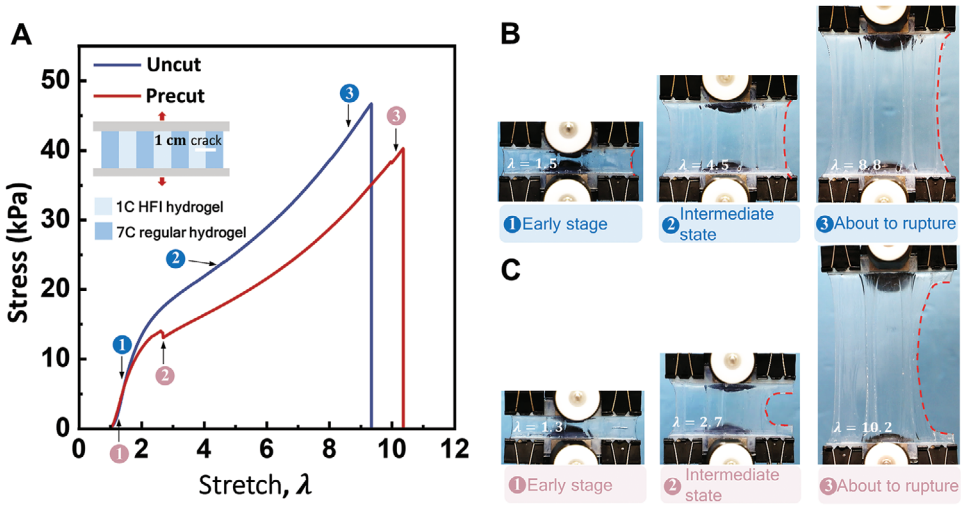

Figure 5. Highly flaw-insensitive soft composites enabled by the HFI PAAm hydrogels. A) Stress–stretch curves of uncut and precut soft composites consisting of alternating strips of 1C HFI hydrogel and 7C regular hydrogel. The comparison of stretchability between soft composites with and without the 1 cm flaw demonstrates great flaw insensitivity of the soft composite. B,C) Snapshots of uncut and precut soft composite under stretch. The snapshots are corresponding to particular moments on the stress–stretch curves.

alternating pattern (inset of **Figure** 5A). The soft composite consists of seven hydrogel stripes with an overall dimension of 8 cm × 1 cm. A 1 cm flaw is introduced in the sample—across the interface of two adjacent strips—to evaluate the flaw-sensitivity of the soft composite. For a composite sample without any flaw, it ruptures at a stretch ratio of 9.3 (Figure 5A,B). In contrast, when the soft composite with the 1 cm flaw is stretched, the regular hydrogel strip ruptures at the stretch of 2.7 due to flaw extension, while the flaw extension is halted by the neighboring HFI hydrogel strip (Figure 5C). The soft composite preserves its stretchability and ruptures until $\lambda_r = 10.4$, even slightly higher than that of uncut soft composite, showing that the soft composite is insensitive to the 1 cm flaw. These results highlight the reinforcement effect of the HFI hydrogel on other regular hydrogels, and demonstrate its potential for fabricating soft composites with high flaw insensitivity.

The strategy of synthesizing highly flaw-insensitive PAAm hydrogel is also applicable for other hydrogels. Following similar approaches, we fabricate poly(N,N-dimethylacrylamide) hydrogels (PDMA hydrogels, an extensively used biocompatible hydrogel) using an unusually low amount of crosslinkers $C = 0.1144 \times 10^{-4}$, resulting in PDMA networks of widely distributed chain lengths. Large-sized PDMA samples with in-plane dimensions of 20 cm (width) × 2 cm (height) and 20 cm (width) × 3 cm (height) are used to test the flaw-sensitivity of the PDMA hydrogel. Both samples exhibit flaw-insensitive behaviors (Figure S21, Supporting Information). For example, for the 20 cm (width) × 3 cm (height) PDMA hydrogel, the intact samples can be stretched until $\lambda_r = 38.29$, while the precut sample with a 10 cm flaw ruptures at a larger stretch, $\lambda_r = 41.43$. The results demonstrate that the PDMA hydrogel also possesses high flaw insensitivity, indicating the broad applicability of the strategy.

Finally, we would like to mention that PAAm hydrogels with extremely low crosslinking density have also been studied in other research works, representative examples include studies of Kim et al.[5a] and Norioka et al.[30] Our study is unique in terms of synthesis processes and mechanical properties compared to that of Kim et al. and in terms of discoveries and understandings compared to that of Norioka et al. Kim et al. synthesized the PAAm hydrogel using a precursor with an uncommonly low water content (≈34 wt%), which produces dense entanglements that are ten times higher than the HFI hydrogels in our work in terms of the entanglement-to-crosslink ratio. The resulting massive amounts of entanglements reduce effective chain lengths and significantly increase the friction between polymer chains, leading to a millimeter-scale fractocohesive length of their hydrogel. The hydrogel studied by Norioka et al. with a crosslinker concentration of $C = 0.1 \times 10^{-4}$ is similar to that of our HFI hydrogel on the aspect of material formulation. However, they do not investigate the fracture behavior of the hydrogel, which should be tested using precut samples according to the fracture mechanics principle. As a result, the remarkable flaw-insensitivity and record-breaking centimeter-scale fractocohesive length of the hydrogels—the key findings of our work—are not reported in their work. The key synergistic mechanism underpinning the inelastic crack blunting and the resulting high flaw insensitivity are not revealed in their work either.

3. Conclusions

In summary, we have synthesized a highly flaw-insensitive PAAm hydrogels containing an entangled inhomogeneous network of unequal chain lengths, using an unusually low amount of crosslinkers. The hydrogels achieve a fractocohesive length up to 2.21 cm, which sets the highest record for synthetic hydrogels and exceeds that of most hydrogels—including regular PAAm hydrogels—by more than one order of magnitude. The HFI hydrogels also possess centimeter-scale flaw-insensitive length (another material constant that quantitatively measures the flaw sensitivity of materials), well exceeding reported values of flaw-insensitive length for typical soft materials that range from several micrometers to several millimeters. The unprecedented flaw

insensitivity stems from the inelastic deformation resulting from a combination of mechanisms including i) coiled long chains, ii) widely distributed chain lengths, iii) moderate amounts of entanglements, and iv) sliding between long chains lubricated by water molecules. When the hydrogel is stretched, the short chains break, while the coiled long chains disentangled and—"lubricated" by the high content of water—slide against each other to unwind and straighten, which collectively generates inelastic deformation. The large inelastic deformation at the crack tip leads to pronounced inelastic crack blunting, which deconcentrates the stress near the crack tip and blocks the extension of the crack. Owing to the large fractocohesive length, HFI hydrogel samples with characteristic lengths of several centimeters are insensitive to flaws contained in the sample. We further show that the strategy of synthesizing HFI hydrogels can be readily extended to other hydrogel systems such as PDMA hydrogels. Despite the unusually low amount of crosslinker used, the modulus of synthesized HFI hydrogel, counter-intuitively, is not compromised because of topological entanglements formed. In terms of applications, the HFI hydrogels can be combined with regular hydrogels to fabricate flaw-insensitive soft composites. It is hoped that the HFI hydrogels will aid in bioengineering and soft robotics.

Supporting Information

Supporting Information is available from the Wiley Online Library or from the author.

Acknowledgements

The authors gratefully acknowledge the financial support from the National Key Technologies Research and Development Program (Grant No. 2022YFC3203900), Natural Science Foundation of Zhejiang Province (Grant No. LR22A020005 and LR23A020001), the National Natural Science Foundation of China (Grant No. 12321002, 12072314, 12002304, and 12272337), the 111 Project (Grant No. B21034), Laoshan Laboratory (Grant No. LSKJ202205300), and the Key Research and Development Project of Zhejiang Province (Grant No. 2022C01022, 2023C03007).

Conflict of Interest

The authors declare no conflict of interest.

Author Contributions

J.M. and X.Z.Z. contributed equally to this work. J.M. synthesized the samples, conducted the experiments, processed and analyzed the data, and co-wrote the manuscript. X.Z.Z. carried out the molecular dynamics simulations and co-wrote the manuscript. D.C.Y. conducted the experiments of PDMA hydrogels. S.Z.Z. designed the study, co-wrote and revised the manuscript. Z.J. designed the study, conceived the idea, supervised the project, co-wrote and revised the manuscript. All authors discussed the results.

Data Availability Statement

The data that support the findings of this study are available from the corresponding author upon reasonable request.

Keywords

flaw-insensitive length, flaw-insensitivity, fractocohesive length, hydrogels, inelastic crack blunting

Received: November 7, 2023
Revised: March 3, 2024
Published online:

[1] a) Y. Guo, F. Yin, Y. Li, G. Shen, J.-C. Lee, *Adv. Mater.* **2023**, *35*, 2300855; b) J. Zhang, Q. Jia, Z. Yue, J. Huo, J. Chai, L. Yu, R. Nie, H. Shao, Y. Zhao, P. Li, W. Huang, *Adv. Mater.* **2022**, *34*, 2200334.
[2] a) M. F. B. Jamaluddin, A. Ghosh, A. Ingle, R. Mohammed, A. Ali, M. Bahrami, G. Kaiko, Z. Gibb, E. C. Filipe, T. R. Cox, A. Boulton, R. O'Sullivan, Y. Ius, A. Karakoti, A. Vinu, P. Nahar, K. Jaaback, V. Bansal, P. S. Tanwar, *Proc. Natl. Acad. Sci. USA.* **2022**, *119*, 2208040119; b) R. Edri, I. Gal, N. Noor, T. Harel, S. Fleischer, N. Adadi, O. Green, D. Shabat, L. Heller, A. Shapira, I. Gat-Viks, D. Peer, T. Dvir, *Adv. Mater.* **2019**, *31*, 1803895.
[3] a) A. Pantula, B. Datta, Y. Shi, M. Wang, J. Liu, S. Deng, N. J. Cowan, T. D. Nguyen, D. H. Gracias, *Sci. Rob.* **2022**, *7*, eadd2903; b) J. Ko, C. Kim, D. Kim, Y. Song, S. Lee, B. Yeom, J. Huh, S. Han, D. Kang, J.-S. Koh, J. Cho, *Sci. Rob.* **2022**, *7*, eabo6463.
[4] a) J.-Y. Sun, X. Zhao, W. R. K. Illeperuma, O. Chaudhuri, K. H. Oh, D. J. Mooney, J. J. Vlassak, Z. Suo, *Nature.* **2012**, *489*, 133; b) J. P. Gong, Y. Katsuyama, T. Kurokawa, Y. Osada, *Adv. Mater.* **2003**, *15*, 1155; c) M. Zhang, Y. Yang, M. Li, Q. Shang, R. Xie, J. Yu, K. Shen, Y. Zhang, Y. Cheng, *Adv. Mater.* **2023**, *35*, 2301551.
[5] a) J. Kim, G. Zhang, M. Shi, Z. Suo, *Science.* **2021**, *374*, 212; b) M. Shi, J. Kim, G. Nian, Z. Suo, *Extreme Mech. Lett.* **2023**, *59*, 101953; c) P. Liu, Y. Zhang, Y. Guan, Y. Zhang, *Adv. Mater.* **2023**, *35*, 2210021.
[6] Z. Wang, X. Zheng, T. Ouchi, T. B. Kouznetsova, H. K. Beech, S. Av-Ron, T. Matsuda, B. H. Bowser, S. Wang, J. A. Johnson, J. A. Kalow, B. D. Olsen, J. P. Gong, M. Rubinstein, S. L. Craig, *Science.* **2021**, *374*, 193.
[7] M. Hua, S. Wu, Y. Ma, Y. Zhao, Z. Chen, I. Frenkel, J. Strzalka, H. Zhou, X. Zhu, X. He, *Nature.* **2021**, *590*, 594.
[8] a) Y. Hong, Y. Chi, S. Wu, Y. Li, Y. Zhu, J. Yin, *Nat. Commun.* **2022**, *13*, 530; b) J. Steck, J. Kim, Y. Kutsovsky, Z. Suo, *Nature.* **2023**, *624*, 303.
[9] a) L. Zeng, F. Liu, Q. Yu, C. Jin, J. Yang, Z. Suo, J. Tang, *Sci. Adv.* **2023**, *9*, eade7375; b) Y. Yang, X. Wang, F. Yang, H. Shen, D. Wu, *Adv. Mater.* **2016**, *28*, 7178; c) W. Li, L. Li, S. Zheng, Z. Liu, X. Zou, Z. Sun, J. Guo, F. Yan, *Adv. Mater.* **2022**, *34*, 2203049.
[10] a) C. Chen, Z. Wang, Z. Suo, *Extreme Mech. Lett.* **2017**, *10*, 50; b) C. Yang, T. Yin, Z. Suo, *J. Mech. Phys. Solids.* **2019**, *131*, 43; c) J. Liu, C. Yang, T. Yin, Z. Wang, S. Qu, Z. Suo, *J. Mech. Phys. Solids.* **2019**, *133*, 103737; d) S. R. Lavoie, Z. Suo, *Math. Mech. Solids.* **2023**, 10812865231208174.
[11] B. Xue, Z. Bashir, Y. Guo, W. Yu, W. Sun, Y. Li, Y. Zhang, M. Qin, W. Wang, Y. Cao, *Nat. Commun.* **2023**, *14*, 2583.
[12] S. Lin, X. Liu, J. Liu, H. Yuk, H.-C. Loh, G. A. Parada, C. Settens, J. Song, A. Masic, G. H. McKinley, X. Zhao, *Sci. Adv.* **2019**, *5*, eaau8528.
[13] a) J. Tang, J. Li, J. J. Vlassak, Z. Suo, *Extreme Mech. Lett.* **2017**, *10*, 24; b) R. Bai, Q. Yang, J. Tang, X. P. Morelle, J. Vlassak, Z. Suo, *Extreme Mech. Lett.* **2017**, *15*, 91.
[14] B. Yiming, Y. Han, Z. Han, X. Zhang, Y. Li, W. Lian, M. Zhang, J. Yin, T. Sun, Z. Wu, T. Li, J. Fu, Z. Jia, S. Qu, *Adv. Mater.* **2021**, *33*, 2006111.
[15] Y. Kamiyama, R. Tamate, T. Hiroi, S. Samitsu, K. Fujii, T. Ueki, *Sci. Adv.* **2022**, *8*, eadd0226.
[16] Y. Zhou, J. Hu, P. Zhao, W. Zhang, Z. Suo, T. Lu, *J. Mech. Phys. Solids.* **2021**, *153*, 104483.

[17] J. Li, W. R. Illeperuma, Z. Suo, J. J. Vlassak, *ACS Macro Lett.* **2014**, *6*, 520.
[18] a) W. Cui, D. R. King, Y. Huang, L. Chen, T. L. Sun, Y. Guo, Y. Saruwatari, C.-Y. Hui, T. Kurokawa, J. P. Gong, *Adv. Mater.* **2020**, *32*, 1907180; b) D. C. Drucker, J. R. Rice, *Eng. Fract. Mech.* **1970**, *1*, 577.
[19] Y. Wang, G. Nian, J. Kim, Z. Suo, *J. Mech. Phys. Solids.* **2023**, *170*, 105099.
[20] Y. Wang, T. Yin, Z. Suo, *J. Mech. Phys. Solids.* **2021**, *150*, 104348.
[21] B. Bao, Q. Zeng, K. Li, J. Wen, Y. Zhang, Y. Zheng, R. Zhou, C. Shi, T. Chen, C. Xiao, B. Chen, T. Wang, K. Yu, Y. Sun, Q. Lin, Y. He, S. Tu, L. Zhu, *Nat. Mater.* **2023**, *22*.
[22] R. E. Shadwick, A. P. Russell, R. F. Lauff, *Philos. Trans. R. Soc. London, B.* **1992**, *337*, 419.
[23] K. Bircher, M. Zündel, M. Pensalfini, A. E. Ehret, E. Mazza, *Nat. Commun.* **2019**, *10*, 792.
[24] X. Chen, J. Lin, H. Yang, J. Tang, *Extreme Mech. Lett.* **2024**, *67*, 102129.
[25] D. Ahmad, K. Patra, M. Hossain, *Continuum Mech. Thermodyn.* **2020**, *32*, 489.
[26] a) J. E. Mark, *Macromol. Symp.* **2003**, *191*, 121; b) S. D. Gehman, *Rubber Chem. Technol.* **1969**, *42*, 659; c) W. F. Watson, *Trans. Faraday Soc.* **1953**, *49*, 1369; d) W. F. Watson, *Trans. Faraday Soc.* **1953**, *49*, 842; e) M. Tao, S. Lavoie, Z. Suo, M. K. Cameron, *Extreme Mech. Lett.* **2023**, *61*, 102024; f) P. Sun, S. Qu, R. Xiao, *J. Mech. Phys. Solids.* **2024**, *184*, 105543.
[27] T. Kopač, A. Ručigaj, M. Krajnc, *Int. J. Biol. Macromol.* **2020**, *159*, 557.
[28] a) S. Hassan, J. Kim, Z. suo, *J. Mech. Phys. Solids.* **2022**, *158*, 104675; b) J. Steck, J. Kim, J. Yang, S. Hassan, Z. Suo, *Extreme Mech. Lett.* **2020**, *39*, 100803.
[29] a) B. Liu, T. Yin, J. Zhu, D. Zhao, H. Yu, S. Qu, W. Yang, *Proc. Natl. Acad. Sci. USA.* **2023**, *120*, 2217781120; b) F. Wang, R. A. Weiss, *Macromolecules.* **2018**, *51*, 7386; c) W. Zhang, J. Hu, J. Tang, Z. Wang, J. Wang, T. Lu, Z. Suo, *ACS Macro Lett.* **2019**, *8*, 17.
[30] C. Norioka, Y. Inamoto, C. Hajime, A. Kawamura, T. Miyata, *NPG Asia Mater.* **2021**, *13*, 34.